Endothelial protein C receptor–expressing hematopoietic stem cells reside in the perisinusoidal niche in fetal liver

Hiroko Iwasaki,[1] Fumio Arai,[1] Yoshiaki Kubota,[1] Maria Dahl,[2] and Toshio Suda[1]

[1]Department of Cell Differentiation, The Sakaguchi Laboratory of Developmental Biology, Keio University School of Medicine, Tokyo, Japan; and [2]Molecular Medicine and Gene Therapy, Lund Stem Cell Center, Lund University, Lund, Sweden

Hematopoietic stem cells (HSCs) are maintained in specialized niches in adult bone marrow. However, niche and HSC maintenance mechanism in fetal liver (FL) still remains unclear. Here, we investigated the niche and the molecular mechanism of HSC maintenance in mouse FL using HSCs expressing endothelial protein C receptor (EPCR). The antiapoptotic effect of activated protein C (APC) on EPCR$^+$ HSCs and the expression of protease-activated receptor 1 (Par-1) mRNA in these cells suggested the involvement of the cytoprotective APC/EPCR/Par-1 pathway in HSC maintenance. Immunohistochemistry revealed that EPCR$^+$ cells were localized adjacent to, or integrated in, the Lyve-1$^+$ sinusoidal network, where APC and extracellular matrix (ECM) are abundant, suggesting that HSCs in FL were maintained in the APC- and ECM-rich perisinusoidal niche. EPCR$^+$ HSCs were in a relatively slow cycling state, consistent with their high expression levels of *p57* and *p18*. Furthermore, the long-term reconstitution activity of EPCR$^+$ HSCs decreased significantly after short culture but not when cocultured with feeder layer of FL-derived Lyve-1$^+$ cells, which suggests that the maintenance of the self-renewal activity of FL HSCs largely depended on the interaction with the perisinusoidal niche. In conclusion, EPCR$^+$ HSCs resided in the perisinusoidal niche in mouse FL. (*Blood*. 2010;116(4):544-533)

Introduction

Hematopoietic stem cells (HSCs) are self-renewing multipotent cells that give rise to all hematopoietic lineages throughout life. Their stem cell characteristics are maintained and regulated in a special microenvironment termed the niche.[1] In adult bone marrow (BM), 2 types of HSC niches have been identified: the osteoblastic niche and the vascular niche.[2] In the osteoblastic niche, osteoblasts and surrounding stromal components in the endosteum region regulate long-term HSCs (LT-HSCs) via cell adhesion and cytokine-mediated signaling.[3-7] The vascular niche consists of sinusoidal endothelial cells (ECs) and reticular cells that secrete CXCL12, which is a chemokine that promotes HSC maintenance.[8,9] HSCs maintain cell-cycle quiescence via the interaction with these niches. In contrast with the adult stage, the fetal liver (FL) is a main hematopoietic organ during development in mid-late gestation, where HSCs are rapidly self-renewed to secure an HSC pool that is sufficient for postnatal life.[10] Unlike what is observed for adult BM, the microenvironment of FL and the molecular mechanism that underlies HSC expansion and maintenance are largely unknown.

Endothelial protein C receptor (EPCR, *Procr*) is a type I transmembrane glycoprotein[11] expressed mainly in ECs of larger blood vessels, liver sinusoids, monocytes, leukocytes, and several tumor cells.[12-16] The major role of EPCR is anticoagulation. EPCR binds to protein C with high affinity and augments the activation of protein C by thrombin-thrombomodulin (TM) complex.[17] Released activated protein C (APC) binds to cofactor protein S and degrades the coagulation factors Va and VIIIa. Another important functional aspect of EPCR is its cytoprotective action. EPCR-bound APC induces signaling that is mediated by the protease-activated receptor 1 (Par-1).[18] This APC/EPCR/Par-1 pathway exerts multiple activities, which include antiapoptosis,[19,20] anti-inflammatory action,[21] and anti–endothelial barrier activation.[22] The expression of *Procr* in HSCs was first observed during the exploration of the nonhematopoietic gene profile using DNA microarray technology.[23] Recent studies showed that EPCR can be used as a tool to identify LT-HSCs, or to purify signaling lymphocytic activation molecule (CD48$^-$CD150$^+$) HSCs.[24,25] However, whether EPCR has a functional role in HSC maintenance or regulation remains to be elucidated.

Achieving ex vivo expansion of HSCs is clinically important for securing a stable and readily available source of HSCs for transplantation. FL-derived HSCs are a good candidate for this purpose because of their distinct capabilities in the in utero treatment of severe immunologic, hematologic, and metabolic diseases.[26] The understanding of the biology of developing FL-derived HSCs and the identification of the HSC niche in FL and of the molecular mechanism that governs HSC maintenance are crucial not only for the treatment of these difficult cases, but also for the development of novel therapeutic protocols for HSC transplantation and for artificial generation of HSCs. In this study, we attempted to identify the HSC niche in FL and the molecular mechanism of FL HSC maintenance through the investigation of the nature of EPCR$^+$ HSCs in embryonic day 12.5 (E12.5) mouse FL. We showed that lineage-negative (Lin$^-$) Sca-1$^+$c-Kit$^+$ (LSK) EPCR$^+$ cells but not EPCR$^-$ cells possessed HSC characteristics. The expression of the Par-1 mRNA and the antiapoptotic effect of APC on LSK/EPCR$^+$ cells suggest the involvement of the APC/EPCR/Par-1 pathway in EPCR$^+$ HSC maintenance. FL-derived LSK cells are rapidly expanding cells, but the EPCR$^+$ fraction was

Submitted August 28, 2009; accepted April 23, 2010. Prepublished online as *Blood* First Edition paper, May 4, 2010; DOI 10.1182/blood-2009-08-240903.

The online version of this article contains a data supplement.

The publication costs of this article were defrayed in part by page charge payment. Therefore, and solely to indicate this fact, this article is hereby marked "advertisement" in accordance with 18 USC section 1734.

in a relatively slow cycling state and contained a higher number of cells in the G0/G1 phase, compared with the EPCR$^-$ fraction. Immunohistochemistry revealed that EPCR$^+$ HSCs were localized in the APC-rich and extracellular matrix (ECM)–rich Lyve-1$^+$ perisinusoidal region. LT reconstitution activity of LSK/EPCR$^+$ cells significantly decreased after short-term culture, but not when cocultured with feeder layer of FL-derived Lyve-1$^+$ cells, which suggests that the maintenance of the self-renewal activity of FL HSCs was largely dependent on the interaction with this perisinusoidal niche. EPCR$^+$ HSC resided in the perisinusoidal niche in mouse FL where the cytoprotective function of EPCR contributed to the maintenance of EPCR$^+$ HSCs.

Methods

Animals

Ly5.1 and Ly5.2 adult female C57/BL6 mice, pregnant or nonpregnant, were purchased from Sankyo Labo Service Corporation. To obtain FL, pregnant mice were killed at E12.5, and embryos were dissected. Femurs and tibias were used for BM analysis. Animals were handled according to the Guidelines for the Care and Use of Laboratory Animals of Keio University School of Medicine with the approval of the institutional review board of Keio University.

FL cell isolation and sorting

Mononuclear cells obtained from FL were blocked with an anti-CD16/32 (clone 93) antibody (BioLegend), followed by predepletion of differentiated hematopoietic cells with autoMACS (Miltenyi Biotec). Used antibodies are indicated in the supplemental Methods (available on the *Blood* Web site; see the Supplemental Materials link at the top of the online article). Lin$^-$ cells were further stained with biotinylated anti–EPCR (clone RMEPCR1560; StemCell Technologies) and other markers indicated (supplemental Methods). A BD FACSVantage system and the FACSDiva software (BD Biosciences) were used to perform flow cytometric analysis and cell sorting.

Colony-forming unit assay

Six hundred sorted LSK/EPCR$^+$ or LSK/EPCR$^-$ cells were suspended in 3 mL of MethoCult GF M3434 medium (StemCell Technologies), distributed into three 35-mm dishes, and then incubated in 5% CO_2 at 37°C. The number and type of colonies were monitored for up to 15 days using a Nikon TMS inverted phase-contrast microscope (Nikon).

Long-term competitive BM reconstitution assay

LSK/EPCR$^+$ or LSK/EPCR$^-$ cells derived from Ly5.1 E12.5 mouse FL were sorted and transplanted (2×10^3 cells/recipient) intravenously into the tail vein of lethally irradiated Ly5.2 recipient mice, together with Ly5.2 BM-derived unfractionated mononuclear competitor cells (2×10^5 cells/recipient). Peripheral blood cells were analyzed every month after transplantation for Ly5.1 and Ly5.2 chimerism using flow cytometry. HSC capacity of transplanted LSK/EPCR$^+$ cells in engrafted BM was analyzed for the presence of LSK fraction, myeloid, lymphoid, and erythroid lineages 4 months after transplantation. For serial BM transplantation, unfractionated mononuclear BM cells were isolated from primary recipient mice 3 months after the primary transplantation and injected (1×10^6 cells/recipient) into lethally irradiated Ly5.2 recipient mice.

RT-PCR analysis

Total RNA was extracted using the RNeasy Mini Kit (Qiagen). The Advantage RT-for-PCR Kit (Clontech Laboratories) or the Transcriptor High-Fidelity cDNA Synthesis Kit (Roche Diagnostics) was used for cDNA synthesis. Ex Taq, dNTP Mixture, and Ex Taq Buffer (Takara Bio) were used for reverse transcription (RT). The primer sequences used for the RT of TM (*Thbd*) and Par-1 (*F2r*) were as follows: 5′–*Thbd* (GCTTTTCTCGGAACTTGCAC), 3′–*Thbd* (TGGTGTGGTTATCGCCAGTA), 5′–*F2r* (GGTGTGCTACACGTCCATCAT), and 3′–*F2r* (AGCACAAGATGCTGTAGAGGT). *Gapdh* (Applied Biosystems) was used as an internal control.

Culture assay with APC supplement

Sorted LSK/EPCR$^+$ and LSK/EPCR$^-$ cells (5000 cells/well) were incubated in 5% CO_2 at 37°C in 200 μL of serum-free SF-O3 medium (Sanko Junyaku) supplemented with recombinant murine stem cell factor (SCF), recombinant human thrombopoietin (Tpo, 0.1 μg/mL each; Wako Pure Chemical Industries), 100 to 1000nM recombinant human APC drotrecogin alfa activated (Xigris; Eli Lilly and Company) on a U-bottom, fibronectin-coated, 96-well plate (AGC Techno Glass). The activity of human APC in mice was verified previously.[27] After 2 days, cells were collected and stained with 0.4% trypan blue solution (Invitrogen) for cell death quantification. Cells were counted manually using the OneCell Counter (OneCell).

Immunohistochemistry

Immunohistochemistry was performed using frozen E12.5 embryo. Detailed procedures of section preparation, staining protocol, and antibodies used are indicated in the supplemental Methods.

Cell-cycle analysis

For cell-cycle analysis using flow cytometry, BrdU and Ki67 assay systems were used. Detailed procedure is described in the supplemental Methods.

High-throughput quantitative RT-PCR analysis

cDNA was synthesized as described in "RT-PCR analysis" and processed as previously described.[28] TaqMan Universal PCR Master Mix (Applied Biosystems), TaqMan Gene Expression Assays (Applied Biosystems), 48.48 Dynamic Array, and BioMark System (Fluidigm) were used to perform polymerase chain reaction (PCR). *Actb* was used as an internal control. The BioMark Real-Time PCR Software (Fluidigm) was used for data analysis.

Short-term culture in serum-free medium

For short-term culture before transplantation, LSK/EPCR$^+$ cells derived from Ly5.1 E12.5 mouse FL were sorted and 1.7×10^4 cells/well were incubated in 200 μL of serum-free SF-O3 medium supplemented with recombinant murine SCF and recombinant human Tpo (0.1 μg/mL each) on a RetroNectin-coated 96-well plate in 5% CO_2 at 37°C (RetroNectin; Takara Bio). Two days later, cells were collected and prepared for injection into lethally irradiated Ly5.2 recipient mice, together with competitive cells, as described earlier. LSK/EPCR$^+$ and LSK/EPCR$^-$ cells derived from E12.5 mouse FL were sorted for short-term culture before gene expression analysis (5×10^3 cells/well), cell-cycle analysis, and apoptosis assay (1.1×10^4 cells/well). Cells were incubated in 200 μL of serum-free SF-O3 medium supplemented with recombinant murine SCF and recombinant human Tpo (0.1 μg/mL each), on a fibronectin-coated 96-well plate (AGC Techno Glass). Cells were collected 1 and 2 days later for gene expression assay and cell-cycle/apoptosis assays, respectively. For coculture, FL-derived CD45$^-$Ter119$^-$Lyve-1$^+$ feeder cells were sorted and precultured for 5 days on a gelatin-coated 96-well plate in endothelial serum-free medium (Invitrogen) supplemented with recombinant human fibroblast growth factor (R&D Systems) and recombinant mouse insulin-like growth factor II (R&D Systems), according to the manufacturer's instructions. LSK/EPCR$^+$ cells were plated on the feeder cells and culture for another day, and then prepared for injection as described earlier. Control cells were cultured in the same medium and condition but without the feeder cells.

Apoptosis assay

After short-term culture, cells were collected and stained with surface markers, followed by annexin V (BD Biosciences) staining along with

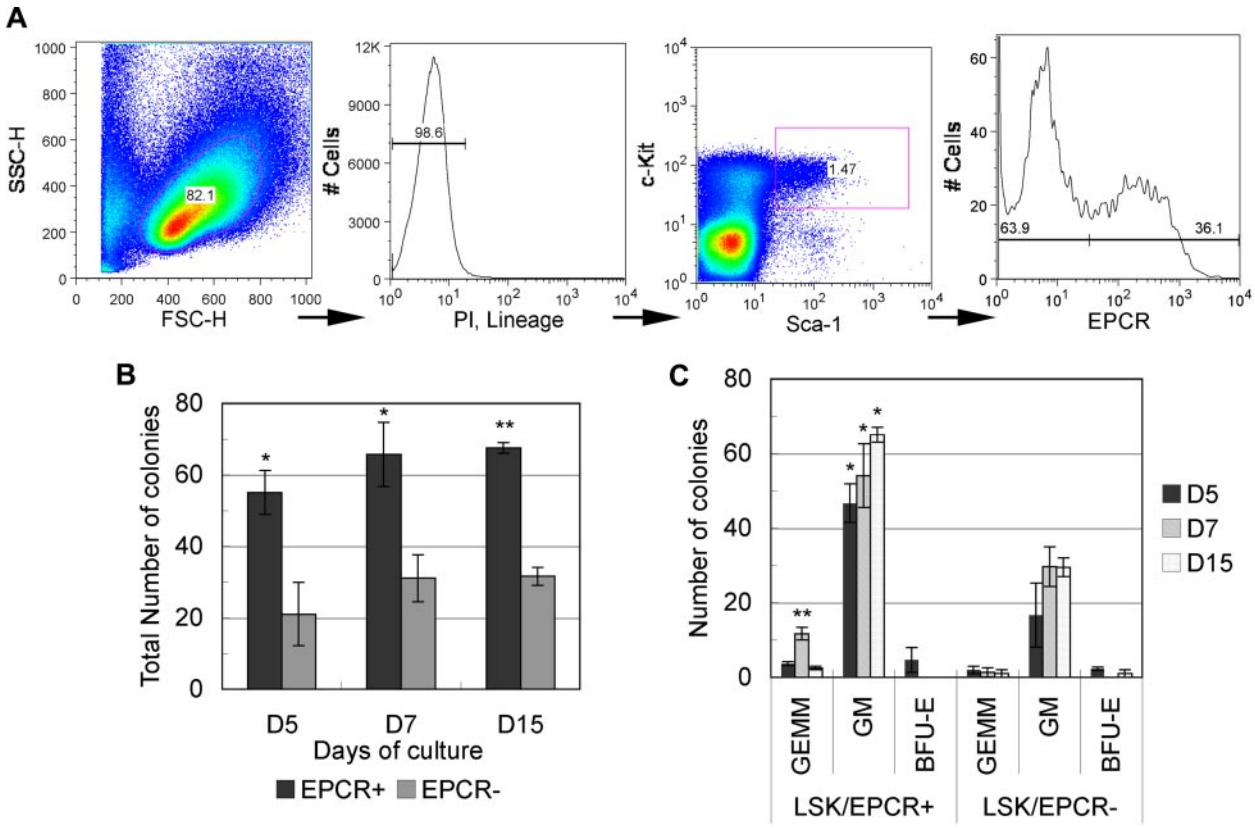

Figure 1. Isolation of LSK/EPCR$^+$ cells using flow cytometric and CFU-C analysis. (A) After mature blood cell lineage predepletion, E12.5 mouse FL cells were gated against viable immature hematopoietic cells. Subsequently, the LSK fraction was determined and was subdivided into EPCR$^+$ and EPCR$^-$ fractions. Sorted LSK/EPCR$^+$ and LSK/EPCR$^-$ cells were submitted to CFU-C analysis. LSK/EPCR$^+$ cells formed a significantly higher number of colonies at all observation stages (B), as well as a larger variety of colonies (C). Error bars represent SD (n = 3). *$P < .05$, **$P < .01$.

the DNA staining with 4′,6-diamidino-2-phenylindole, and analyzed with a flow cytometer.

Statistics

Results are shown as mean plus or minus SD. The Student *t* test, Tukey test, and Dunnett test were used to evaluate the significance of results.

Results

LSK/EPCR$^+$ cells in FL represented a stem/progenitor cell–rich fraction with a higher colony-forming unit activity and contained immature cells

To examine the hematopoietic potential of EPCR$^+$ cells, we performed a colony-forming unit cell (CFU-C) assay. Differentiated hematopoietic cell–depleted mononuclear cells were gated into an immature hematopoietic stem/progenitor LSK fraction using a flow cytometer and were then subdivided into EPCR$^+$ and EPCR$^-$ fractions (Figure 1A). Roughly 30% of LSK cells were EPCR$^+$ (32.1 ± 3.2%, n = 3). The CFU-C assay was performed on both EPCR$^+$ and EPCR$^-$ cells in a medium containing cytokines that promoted multiple-lineage differentiation. Throughout the monitoring period (up to 15 days), EPCR$^+$ cells consistently formed a significantly higher number of colonies compared with EPCR$^-$ cells (Figure 1B). In addition, EPCR$^+$ cells formed a higher number of burst-forming unit erythroid (BFU-E)–derived colonies and CFU granulocyte erythrocyte monocyte macrophage (CFU-GEMM)–derived colonies, whereas EPCR$^-$ cells resulted in few GEMM- and BFU-E–derived colonies (Figure 1C). These data suggest that the LSK/EPCR$^+$ fraction contains a greater number of stem/progenitor cells with higher differentiation potential.

LSK/EPCR$^+$, but not EPCR$^-$, cells exhibited long-term BM reconstitution activity

We examined the capacity of LSK/EPCR$^+$ cells to act as HSCs in vivo by investigating their long-term BM reconstitution (LTR) activity. LSK/EPCR$^+$ and LSK/EPCR$^-$ cells were transplanted into lethally irradiated mice. The chimerism of Ly5.1 donor-derived LSK cells was strikingly different between recipients of LSK/EPCR$^+$ and LSK/EPCR$^-$ cells (Figure 2A). LSK/EPCR$^+$ cell recipients showed high donor-derived cell chimerism in the peripheral blood as early as 1 month after transplantation (40.7% ± 8.4%, n = 3), and its proportion increased steadily thereafter (at 3 months, 73.9% ± 7.3%, n = 3). In contrast, the transplantation of LSK/EPCR$^-$ cells led to a chimerism of donor-derived cells that was less than 1% 1 month after transplantation (0.11% ± 0.09%, n = 3) and decreased steadily thereafter (at 3 months, 0.09% ± 0.04%, n = 3). Among the primitive LSK cells, EPCR$^+$ but not EPCR$^-$ cells possessed LTR capacity. To investigate the HSC capacity of the engrafted LSK/EPCR$^+$ cells, donor-derived Ly5.1 cells in recipient BM were analyzed 4 months after the primary transplantation for myeloid, lymphoid, and erythroid lineages as well as LSK fraction using flow cytometry and were compared with untransplanted control mice (Figure 2B). Donor-derived LSK/EPCR$^+$ cells differentiated successfully into all investigated lineages or remained as LSK cells and exhibited an expression pattern similar to control for each of the marker

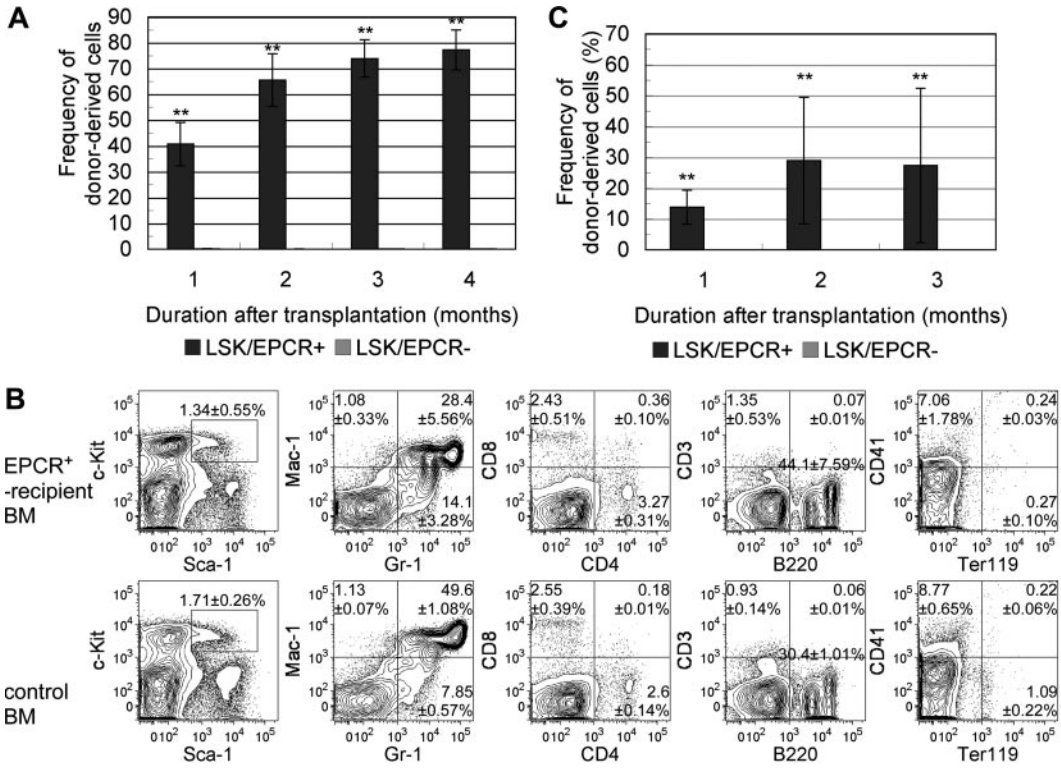

Figure 2. Long-term competitive BM reconstitution assay. (A) LSK/EPCR$^+$ or LSK/EPCR$^-$ cells (2×10^3 cells/recipient) were transplanted into lethally irradiated recipient mice together with BM-derived unfractionated competitor cells (2×10^5 cells/recipient). The chimerism of donor-derived cells in the peripheral blood of recipient mice was significantly higher after transplantation of LSK/EPCR$^+$ cells (■); LSK/EPCR$^-$ cells failed to reconstitute the BM of recipients (□). Error bars represent SD (n = 3). $^{**}P < .01$. (B) Engrafted BM was analyzed 4 months after transplantation for donor-derived LSK fraction, myeloid, lymphoid, and erythroid lineages (top panels). Bottom panels show the data obtained from untransplanted control mice. Representative FACS patterns are shown with data indicating percentage frequency of LSK or population in each quadrant. Data represent mean ± SD (n = 3). (C) Unfractionated BM mononuclear cells were obtained from primary recipients 3 months after transplantation and were transplanted (1×10^6 cells/recipient) into a second set of lethally irradiated recipient mice. Primary donor–derived cells in LSK/EPCR$^+$ recipient mice exhibited BM reconstitution activity with substantial chimerism of peripheral blood cells (■), whereas no such activity was observed when cells from LSK/EPCR$^-$ recipient mice were transplanted (□). Error bars represent SD (n = 5).

combinations. These data suggest that the LSK/EPCR$^+$ cells had full HSC capacity.

Next, we performed secondary transplantation to further determine the long-term repopulating activity of LSK/EPCR$^+$ cells. The unfractionated cells derived from the BM of primary recipients of LSK/EPCR$^+$ or LSK/EPCR$^-$ cells were administered into another set of recipient mice. When the cells from LSK/EPCR$^+$ recipients were transplanted, the primary donor-derived Ly5.1 cells exhibited reconstitution capacity with substantial chimerism of peripheral blood cells, whereas no such activity was observed when the cells from LSK/EPCR$^-$ recipients were transplanted (Figure 2C). This result confirms that only LSK/EPCR$^+$ cells have LTR capacity. Collectively, EPCR$^+$ cells represented a LT-HSC–enriched population in the E12.5 mouse FL-derived LSK fraction.

The APC/EPCR/Par-1 pathway was involved in the maintenance of EPCR-expressing HSCs

TM and Par-1 are indispensable factors, respectively, for the 2 known functions of EPCR (ie, anticoagulant and cytoprotective activities).[17,18] To explore the possibility of EPCR involvement in hematopoiesis, we first examined the mRNA expression of TM and Par-1. TM mRNA was not detected in LSK/EPCR$^+$ or EPCR/LSK$^-$ cells, whereas Par-1 mRNA was abundantly expressed in LSK/EPCR$^+$ cells (Figure 3A), which suggests that TM/EPCR anticoagulant activity is less likely to be involved in the HSC characteristics of LSK/EPCR$^+$ cells. Next, we explored the possibility of the involvement of cytoprotective APC/EPCR/Par-1 pathway activity. Immunohistochemical analysis showed that APC, which is a ligand of EPCR that is essential in the cytoprotective APC/EPCR/Par-1 pathway, was produced in E12.5 mouse FL

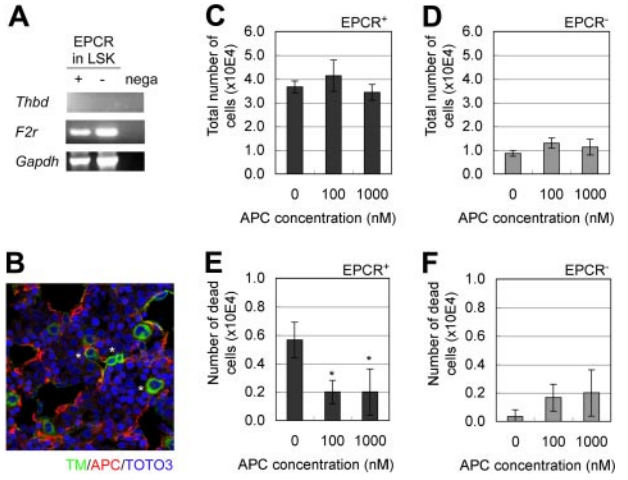

Figure 3. Involvement of the APC/EPCR/Par-1 pathway in the maintenance of EPCR$^+$ HSCs. (A) Both LSK/EPCR$^+$ and LSK/EPCR$^-$ cells expressed the mRNA of Par-1 (*F2r*), but not of TM (*Thbd*). (B) In E12.5 mouse FL, TM-expressing cells (green) shown at asterisk and APC formation (red) were visualized using immunohistochemistry. (C-F) LSK/EPCR$^+$ or LSK/EPCR$^-$ cells were cultured for 2 days in the presence of APC supplementation. The APC supplement did not affect cell proliferation in either LSK/EPCR$^+$ or LSK/EPCR$^-$ cells (C-D); however, it significantly suppressed the number of dead cells among the LSK/EPCR$^+$ population (E). Error bars represent SD (n = 3). $^*P < .05$.

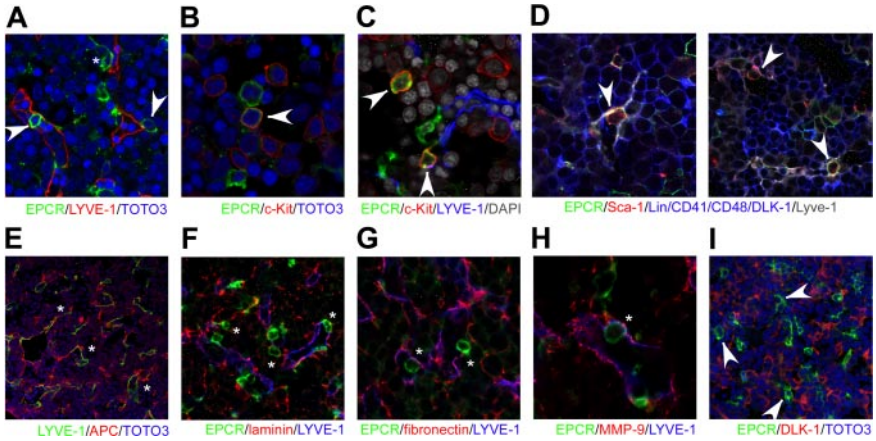

Figure 4. Immunohistochemical analysis of EPCR$^+$ cells in E12.5 mouse FL. (A) EPCR$^+$ cells (green) were detected in E12.5 mouse FL. Some cells were round (arrowheads), and others were spindle-shaped (asterisk). They were observed adjacent or connected to Lyve-1$^+$ sinusoidal ECs (red), both inside and outside of the sinusoid lumen. Magnification is shown at ×120. (B-C) Some c-Kit$^+$ cells (red) coexpressed EPCR (green) shown at arrowheads and located adjacent to the sinusoid (blue). Magnifications are ×240 for panel B and ×180 for panel C. (D) Nonlineage/CD41/CD48/Dlk-1–positive (blue) Sca-1$^+$ (red) EPCR$^+$ (green) cells shown at arrowheads were observed adjacent to the Lyve-1$^+$ sinusoid (gray). Magnifications are ×240 (left) and ×150 (right). (E) APC (red) shown by asterisks distributed along the sinusoid (green) in FL. Magnification is ×40. (F-H) The perisinusoidal region, where EPCR$^+$ cells (green) shown at asterisks are observed, is rich in ECM compounds (red), such as laminin (F), fibronectin (G), and matrix metalloproteinase-9 (MMP-9, H). Magnifications are ×120 for panel E, ×180 for panel F, and ×160 for panel G. (I) No specific spatial interaction was observed between Dlk-1$^+$ hepatoblasts (red) and EPCR$^+$ cells (green), shown at arrowheads. Magnification is ×80.

(Figure 3B). In addition, culture of LSK/EPCR$^+$ and LSK/EPCR$^-$ cells in medium supplemented with APC did not affect the proliferation of either type of cell (Figure 3C-D); however, it significantly reduced the number of dead LSK/EPCR$^+$ cells (Figure 3E-F), which indicates that APC may act as an antiapoptotic mediator in LSK/EPCR$^+$ cells. Collectively, these data suggest that the cytoprotective APC/EPCR/Par-1 pathway was likely to be involved in the maintenance of EPCR$^+$ HSCs.

EPCR$^+$ hematopoietic cells resided in the APC- and ECM-rich perisinusoidal microenvironment in E12.5 mouse FL

To examine the localization of EPCR$^+$ cells, frozen sections were immunostained with anti-EPCR and anti–Lyve-1 antibodies (Figure 4A). Lyve-1 is a lymphatic vessel marker that is also expressed in sinusoidal ECs in the liver.[29] EPCR$^+$ cells were observed adjacent or connected to the sinusoidal EC network, some which were spindle shaped and others which were round shaped. A total of 213 of 229 (92%) EPCR$^+$ cells were connected to the sinusoidal EC network. They were located both inside and outside of the sinusoid lumen. Costaining with c-Kit revealed that some c-Kit$^+$ cells coexpressed EPCR (Figure 4B). EPCR and c-Kit double-positive cells were located adjacent to Lyve-1$^+$ sinusoidal ECs (Figure 4C). Similarly, Lin$^-$CD41$^-$CD48$^-$Dlk-1$^-$Sca-1$^+$ cells were observed adjacent to Lyve-1$^+$ cells, costaining EPCR$^+$ (Figure 4D). APC was distributed abundantly along the sinusoidal network (Figure 4E) and ECM components, such as alpha laminin, fibronectin, and matrix metalloproteinase 9, were also abundant in the area surrounding the sinusoid and EPCR$^+$ cells (Figure 4F-H). Hepatoblasts are the dominating cells in FL; however, no specific spatial interaction of EPCR$^+$ cells with Dlk-1$^+$ hepatoblasts was observed (Figure 4I). These observations suggest that EPCR$^+$ cells were supported by the APC- and ECM-rich Lyve-1$^+$ perisinusoidal microenvironment in E12.5 mouse FL.

LSK/EPCR$^+$ were in a relatively slow cycling state

HSCs in FL undergo rapid self-renewal. Quiescent LT-HSCs in BM are typically characterized by their ability to efflux Hoechst 33342 or rhodamine 123 dye and are detected as a side population (SP) in FACS analysis.[30,31] In contrast, the SP fraction is not detected in FL HSCs.[32] Thus, the precise cell-cycle status of FL HSCs remains unknown.

We investigated cell-cycle status by exposing pregnant mice and their embryos to BrdU in vivo for 2 hours and by performing subsequent analysis of the isolated cells using flow cytometry for anti-BrdU antibody and Hoechst 33342 dye staining. BrdU is an analog of thymidine and is incorporated into the new DNA strand during the S phase.[33] Hoechst 33342 preferentially binds to adenine–thymine-rich regions of the minor groove of DNA and its expression level reflects the amount of DNA.[34] The majority of cells in the LSK/EPCR$^+$ population was in the BrdU$^-$/Hoechst^{low} (G0/G1 phase) fraction and its frequency was significantly higher compared with the LSK/EPCR$^-$ population. In contrast, roughly half of cells in the LSK/EPCR$^-$ population were in the BrdU$^+$ (S phase) fraction, the frequency of which was significantly higher compared with the LSK/EPCR$^+$ population (Figure 5A-B). Ki67 is expressed in the nucleus of cells in all phases of the activated cell cycle but the G0 phase; thus, Ki67 is used often as a proliferation marker.[35] The number of cells in the Ki67$^-$/Hoechst^{low} (G0 phase) and Ki67$^+$/Hoechst^{low} (G1 phase) fractions was higher for the LSK/EPCR$^+$ population than for the LSK/EPCR$^-$ population (Figure 5C). In contrast, the LSK/EPCR$^-$ population exhibited a greater number of cells in the Ki67$^+$/Hoechst^{high} fraction (S/G2/M phase). These results suggest that, in the LSK/EPCR$^+$ population, the cell cycle is delayed at the G0/G1 phase, which was consistent with the BrdU-Hoechst analysis. These data collectively suggest that LSK/EPCR$^+$ cells represented a relatively slow cycling population compared with LSK/EPCR$^-$ cells.

High-throughput quantitative RT-PCR analysis provided a cell-cycle–related gene profile of E12.5 mouse FL-derived LSK cells (Figure 5D). Cyclin-dependent kinase (CDK) inhibitors, such as *p57* and *p18*, were abundantly expressed in LSK/EPCR$^+$ cells, whereas various cell-cycle regulators of G1, G1/S, and G2/M phase progression, such as *Ccnd1*, *Ccnd2*, *Cdk6*, *Cdk2*, and *Aurka*, were expressed in LSK/EPCR$^-$ cells at significantly higher levels. This result reasonably supports the findings that LSK/EPCR$^+$ cells represent a relatively quiescent population with cell-cycle delays at

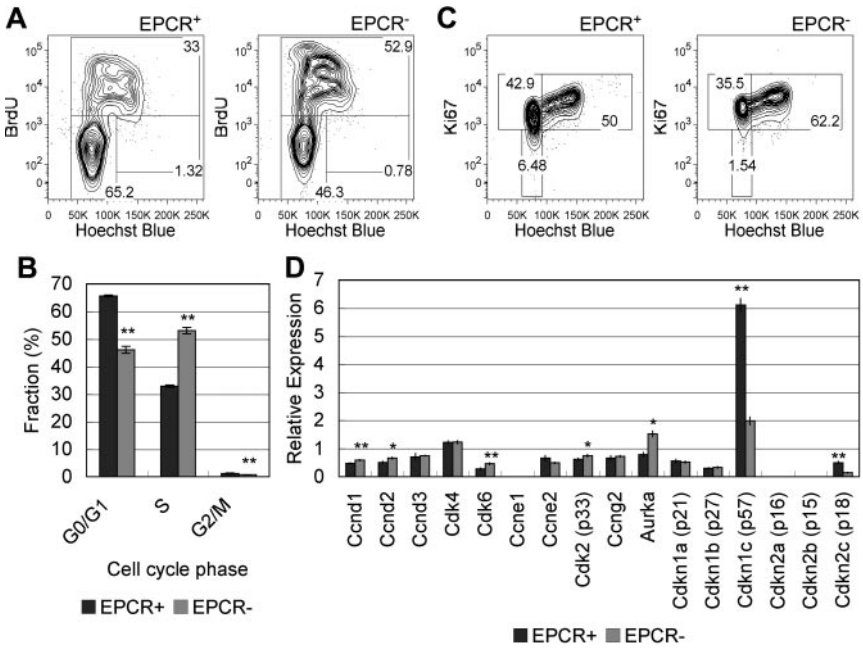

Figure 5. Cell-cycle and mRNA expression analyses in EPCR+ HSCs. (A) E12.5 pregnant mice were exposed to BrdU for 2 hours, and embryos were subsequently analyzed for cell-cycle status. The majority of cells in the LSK/EPCR+ population was in the G0/G1 phase (left) and its frequency was significantly higher compared with the LSK/EPCR− population (right). In contrast, roughly half of the cells in the LSK/EPCR− population were in the S phase (right). (B) Fractions corresponding to each cell-cycle phase were analyzed using the BrdU-Hoechst flow cytometric approach described in panel A. The LSK/EPCR+ (dark gray bars) and LSK/EPCR− (light gray bars) populations are shown. Error bars represent SD (n = 3). $^{**}P < .01$. (C) The LSK/EPCR+ population contained a greater number of cells in the G0 phase than the LSK/EPCR− population, as assessed by Ki67-Hoechst flow cytometry. (D) Cell-cycle–related mRNA expression profile in LSK/EPCR+ and LSK/EPCR− cells, as assessed using a high-throughput quantitative RT-PCR system. LSK/EPCR+ cells expressed significantly higher levels of CDK inhibitors, such as *p57* and *p18*, whereas LSK/EPCR− cells overexpressed CDKs such as *Ccnd1*, *Ccnd2*, *Cdk6*, *Cdk2*, and *Aurka*. The LSK/EPCR+ (■) and LSK/EPCR− (□) populations are shown. Error bars represent SD (n = 3). $^{*}P < .05$, $^{**}P < .01$.

the G0 and G1 phases, and that LSK/EPCR− cells are a relatively proliferative population.

The integrity of LSK/EPCR+ cells as HSCs declined rapidly in vitro

To examine the effect of niche regulation on FL HSC maintenance, E12.5 mouse FL-derived LSK/EPCR+ cells were analyzed after short-term culture. More than 85% of cultured LSK/EPCR+ cells remained Lin−, which is significantly higher than the percentage of cultured LSK/EPCR− cells; however, the remaining LSK and LSK/EPCR+ proportions were small (Figure 6A). Most of the remaining LSK/EPCR+ cells survived from apoptosis (Figure 6B), and their G1 fraction significantly decreased and S/G2/M fraction significantly increased (Figure 6C). LSK/EPCR+ cells cultured for 2 days failed to engraft after transplantation and lost LTR activity (Figure 6D), and the *Procr* expression level was significantly down-regulated (Figure 6E). These data collectively suggest that LSK/EPCR+ cells enter a more proliferative cell-cycle state and start differentiation ex vivo, which resulted in LTR capacity degradation that is no longer recoverable in vivo. To identify genes involved in this rapid degradation of HSC function, the expression levels of 91 hematopoiesis-related genes were analyzed before and after culture of LSK/EPCR+ and LSK/EPCR− cells (supplemental Table 1). Genes were then screened according to the following criteria: (1) there was a significant difference ($P < .1$) in its expression levels between LSK/EPCR+ and LSK/EPCR− cells, and (2) its expression levels in LSK/EPCR+ cells changed significantly ($P < .1$) after culture. Among the genes tested, 3 genes (*Cdk6*, *Cdh5*, and *Sox17*) met these screening criteria (Figure 6F-H).

Cdk6, which encodes cyclin-dependent kinase 6 and is important for cell-cycle G1 phase progression and G1/S phase transition[36] was expressed at a lower level in LSK/EPCR+ cells before culture and was significantly up-regulated after culture (Figure 6F), which indicates that cell-cycle activation was initiated in LSK/EPCR+ cells during the short culture. *Cdh5*, which encodes the EC adhesion molecule vascular endothelial (VE)–cadherin,[37] was expressed dominantly in LSK/EPCR+ cells before culture and was significantly down-regulated after culture (Figure 6G). This suggests that LSK/EPCR+ cells may rely strongly on their surrounding environment, particularly the endothelial microenvironment, to sustain their stem cell capabilities.

The expression levels of *Sox17* were also decreased significantly in LSK/EPCR+ cells during culture (Figure 6H). In addition, we observed that the mRNA levels of *Tcf3* were dramatically decreased in LSK/EPCR+ cells after short culture (supplemental Figure 1A). Sox17 is a transcription factor associated with vascular development and HSC function in early embryonic stages and works as a negative regulator of Dkk1, which is a canonical Wnt signaling antagonist.[38] These results indicate that *Sox17* degradation may have induced a consequent loss of the proliferative capacity of LSK/EPCR+ cells.

Genes involved in cell-ECM adhesion (ie, various types of integrins) showed similar mRNA expression levels in LSK/EPCR+ and LSK/EPCR− cells before short culture, and thus did not meet the screening criteria discussed. It is noteworthy, however, that the mRNA levels of 2 of the integrins tested (ie, *Itga4* and *Itga9*) were significantly down-regulated in LSK/EPCR+ cells exclusively (supplemental Figure 1B-C). These data suggest the possibility that the interaction between the ECM components and integrins expressed in LSK/EPCR+ cells was also involved in HSC maintenance in FL.

HSC capacity of LSK/EPCR+ cells in vitro was sustained in coculture with feeder layer of FL-derived Lyve-1+ cells

To investigate whether FL Lyve-1+ cells play supportive role in maintaining the HSC characteristics of LSK/EPCR+ cells, coculture assay was performed. FL cells were sorted for CD45−Ter119−Lyve-1+ fraction (Figure 7A) and plated in advance. FL Lyve-1+ cells developed into feeder layer in 5 days containing cells with various types of morphologies. LSK/EPCR+ cells were cultured for 1 day with or without feeder layer of FL Lyve-1+ cells and then transplanted into recipient mice. After culture without FL Lyve-1+ feeder cells, posttransplantation LTR activity of LSK/EPCR+ cells was significantly decreased with their constant low chimerisms throughout the 4-month observation

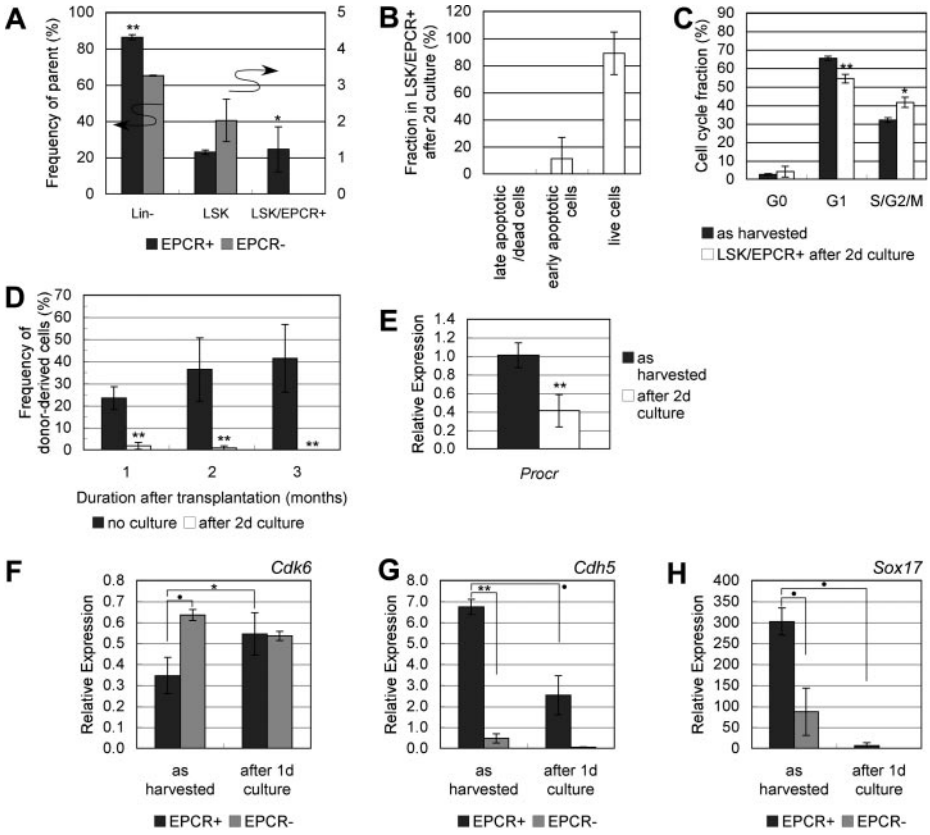

Figure 6. LTR capacity and mRNA expression variation in LSK/EPCR$^+$ cells after short culture. (A) LSK/EPCR$^+$ and LSK/EPCR$^-$ cells underwent short-term culture for 2 days in SF-O3 supplemented with SCF and Tpo, and were analyzed with flow cytometer for remaining Lin$^-$, LSK, and LSK/EPCR$^+$ fractions. A significantly greater population remained in Lin$^-$ fraction in the cultured LSK/EPCR$^+$ cells than in the LSK/EPCR$^-$ cells. A limited proportion of cells remained in LSK and LSK/EPCR$^+$ fractions. The LSK/EPCR$^+$ (■) and LSK/EPCR$^-$ (▩) cells are shown. Error bars represent SD (n = 3). $^*P < .05$, $^{**}P < .01$. (B) Apoptotic status of LSK/EPCR$^+$ fraction remaining after short culture was analyzed. Majority of the remaining LSK/EPCR$^+$ fraction survived from apoptosis. Error bars represent SD (n = 3). (C) Cell-cycle status of remaining LSK/EPCR$^+$ fraction was analyzed after short culture. G1 fraction decreased and S/G2/M fraction increased significantly, compared with those as harvested. LSK/EPCR$^+$ cells (■) represent as harvested. Remaining LSK/EPCR$^+$ cells (□) after short culture are also represented. Error bars represent SD (n = 3). $^*P < .05$, $^{**}P < .01$. (D) LSK/EPCR$^+$ cells were cultured for 2 days in SF-O3 supplemented with SCF and Tpo, and were subsequently transplanted into lethally irradiated recipient mice with BM-derived unfractionated competitor cells. After short culture, cells failed to reconstitute recipient BM. LSK/EPCR$^+$ cells (■) represent as harvested. Cultured LSK/EPCR$^+$ cells (□) are also represented. Error bars represent SD (n = 5). $^{**}P < .01$. (E) EPCR (*Procr*) mRNA levels in LSK/EPCR$^+$ cells decreased significantly during short culture. LSK/EPCR$^+$ cells (■) represent as harvested. Cultured LSK/EPCR$^+$ cells (□) are also represented. Error bars represent SD (n = 3). $^*P < .05$. (F-H) Among the 91 genes tested using high-throughput quantitative RT-PCR, *Cdk6*, *Cdh5*, and *Sox17* were screened based on their significantly different expression levels between LSK/EPCR$^+$ and LSK/EPCR$^-$ cells, as well as on the significant changes in the expression of these genes in EPCR$^+$ cells during short culture. LSK/EPCR$^+$ (■) and LSK/EPCR$^-$ (▩) cells are shown. Error bars represent SD (n = 2). ●$P < .1$, $^*P < .05$, $^{**}P < .01$.

period compared with activity of the freshly transplanted LSK/EPCR$^+$ cells (Figure 7B). On the other hand, chimerism of LSK/EPCR$^+$ cells cultured with FL Lyve-1$^+$ feeder cells was significantly lower initially but started to recover from 2 months after transplantation to the levels statistically equivalent to those of the freshly transplanted LSK/EPCR$^+$ cells. Similarly, donor chimerism in BM 4 months after transplantation was significantly lower in recipients of cells cultured without feeder cells, compared with levels in recipients of freshly transplanted LSK/EPCR$^+$ cells, but no significant difference was observed between the recipients of cells cultured with feeder cells and recipients of freshly transplanted LSK/EPCR$^+$ cells (Figure 7C). Frequency of LSK population showed no significant difference among the 3 kinds of recipients (Figure 7D); however, donor chimerism within LSK population was significantly lower in the recipients of cells cultured without feeder cells, compared with the recipients of freshly transplanted LSK/EPCR$^+$ cells and the recipients of cells cultured with feeder cells (Figure 7E). These data indicate that FL Lyve-1$^+$ feeder cells sustained the LTR activity of LSK/EPCR$^+$ cells that would otherwise have decreased significantly during short culture, suggesting that FL Lyve-1$^+$ cells play a supportive role in maintaining HSC characteristics of LSK/EPCR$^+$ cells.

Discussion

In this study, we demonstrated that the distinctive perisinusoidal region serves as an HSC niche in FL. The LT-HSC characteristics of LSK/EPCR$^+$ cells were largely dependent on the interaction with this perisinusoidal niche. Moreover, a cytoprotective role of EPCR in HSC maintenance and regulation involving the APC/EPCR/Par-1 pathway was suggested.

In adult BM, the osteoblastic niche in the endosteum mainly functions to maintain quiescent LT-HSCs and the vascular niche supports cell-cycle–activated short-term HSCs (ST-HSCs).[2] BM-derived LT-HSCs with LTR activity in vivo also have high proliferative potential in vitro, which is typically observed in long-term culture such as high proliferative potential colony-forming cells assay.[31] Interestingly, our immunohistochemical observation illustrated that sinusoidal ECs and the surrounding APC- and ECM-rich microenvironment serve as an FL niche for LSK/EPCR$^+$ cells that are in a relatively slow cycling state and possess LT-HSC characteristics. Our findings showed that FL-derived HSCs were fragile and quickly lost their LT-HSC capacity

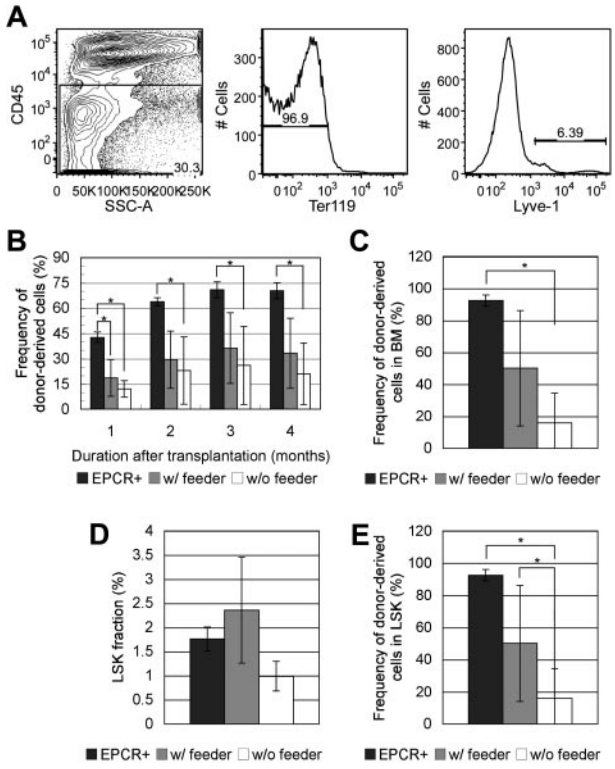

Figure 7. Effect of coculture with FL-derived Lyve-1+ feeder cells on LTR capacity of LSK/EPCR+ cells. (A) FL cells were sorted against CD45−Ter-119−Lyve-1+ fraction. (B) Significantly decreased chimerism of donor-derived LSK/EPCR+ cells in peripheral blood after 1-day culture without feeder cells (□) was recovered when cocultured with feeder layer of FL-derived Lyve-1+ cells (▨) to the levels statistically equivalent to those of freshly transplanted LSK/EPCR+ cells. (C) Chimerism of donor-derived cells in BM 4 months after transplantation decreased significantly when cultured without feeder cells but not when cultured with FL Lyve-1+ feeder cells. (D) Population of LSK fraction 4 months after transplantation showed no statistical difference among the 3 conditions. (E) Chimerism of donor-derived LSK population was significantly decreased in cells cultured without feeder cells and sustained with coculture with FL Lyve-1+ feeder cells. (B-E) Freshly transplanted LSK/EPCR+ cells (■) and LSK/EPCR+ cells cocultured for 1 day with FL Lyve-1+ feeder cells (▨) are shown. LSK/EPCR+ cells cultured without feeder cells (□) are also represented. Error bars represent SD (n = 4 or 5). *$P < .05$.

ex vivo by entering a more proliferative cell-cycle state and starting differentiation, and that coculture with FL Lyve-1+ cells sustained LTR capacity of LSK/EPCR+ cells. This may suggest that the HSC characteristics of LSK/EPCR+ cells were largely dependent on niche components. Various genes have been identified as potential key factors for the maintenance of the stem cell characteristics of LSK/EPCR+ cells. These genes include *Cdk6*, *Cdh5*, and *Sox17*, with the latter 2 being EC-related. This further supports the contention that the integrity of LSK/EPCR+ cells as LT-HSCs depends on the surrounding environment, particularly the sinusoidal endothelial microenvironment. The ECM-integrin interaction plays various roles in cell adhesion, proliferation, morphology, and mobility. In this study, EPCR+ cells were found in an ECM-rich environment, whereas the expression levels of integrin-related mRNA were not significantly distinct between the LSK/EPCR+ and LSK/EPCR− fractions; the degree of variation during short culture was also similar. However, the ECM-integrin interaction includes diverse combinations of molecules and further examination may be necessary to determine whether the ECM-integrin interaction contributes to HSC regulation in FL.

Among the primitive LSK population, only EPCR+ cells have LT-HSC characteristics with LTR and multilineage differentiation capacities. We demonstrated that these LSK/EPCR+ cells were more likely to be in a slow cycling state compared with LSK/EPCR− cells under the regulation of CDK inhibitors such as *p57* and *p18*. Cell-cycle analysis of adult LT-HSCs showed that these cells were in a quiescent state, typically detected as the SP fraction by FACS analysis.[30,31] This feature was confirmed in EPCR+ cells isolated from adult BM.[24] FL HSCs are, in contrast, rapidly expanding cells.[39] Our data indicate that the slowing down of the HSC cell cycle toward the adult stage takes place as early as E12.5, soon after the first appearance of HSCs in FL. Regulation of cell cycle of HSCs in FL, possibly through interaction with perisinusoidal niche, may be critical in development and maintenance of HSCs. In the hepatic sinusoidal development during the murine embryogenesis,[40] primitive sinusoidal structure appears at E10. Hepatic sinusoid does not have basal membrane. At E12 to E14, ECs continuously line the sinusoid, and the space of Disse (the space between endothelium and hepatocytes) is generally narrow. At E15, the lining partially becomes discontinuous and fenestrated, which are the characteristics of sinusoid in adult liver, and the space of Disse gradually widens before birth. Narrow space of Disse and the absence of basal membrane in midgestation must allow the physical contact of ECs with developing hematopoietic cells, presumably helping to furnish perisinusoidal niche for HSCs. The developmental changes in perisinusoidal microenvironment must affect the hematopoietic activity in FL, and be closely linked with the HSCs migration that takes place at E15.5-E16.5. Our quantitative RT-PCR assay screened *Cdh5*, *Cdk6*, and *Sox17* as candidates for key factors of EPCR+ HSC maintenance in perisinusoidal niche in FL. Deletion of *Sox17* leads to dramatic up-regulation of *Dkk1* in HSCs; Dkk1 is a negative regulator of Wnt signaling[38] and Sox17 suppresses the expression of CDK inhibitors, such as *p15*, *p21*, or *p57*, and induces the expression of cell-cycle–promoting genes.[41] These data and our findings collectively indicate that *Sox17* and *Wnt* may work as a cell-cycle promoter mechanism in LSK/EPCR+ cells by maintaining them in the relatively slow but cycling state, thus outcompeting *p57* and *p18*, which are expressed at high levels in LSK/EPCR+ cells. After the degradation of *Sox17*, which is subsequent to short culture, several other factors may initiate cell-cycle progression in LSK/EPCR+ cells. For example, the expression levels of *Gfi1*, which is a cell-cycle break in HSCs,[42] decreased considerably in LSK/EPCR+ cells after short culture (supplemental Figure 1D). VE-cadherin transfers intracellular signals that contribute to antiproliferative responses via transforming growth factor-β signaling.[43] It may play a role in maintaining the relatively quiescent state of LSK/EPCR+ cells in niche in FL. Nevertheless, cell-cycle regulation is a consequence of the delicate balance of various factors and further analysis is required for the complete understanding of this process.

Our data suggest that the cytoprotective APC/EPCR/Par-1 signaling pathway was involved in EPCR+ HSC maintenance in FL. Endothelial-barrier protection is one of the major roles of EPCR, via cooperation with APC-binding Par-1 and sphingosine-1-phosphate receptor 1 (S_1P_1).[22,44] In addition, endogenous APC stimulates the S_1P_1-mediated VE-cadherin–dependent vascular barrier.[45] These findings suggest that the EPCR expressed in LSK cells may contribute to the tight adhesion between LSK/EPCR+ cells and sinusoidal ECs by stimulating VE-cadherin expression via this APC/EPCR/Par-1 signaling pathway. Depletion of EPCR leads to embryonic lethality by E10.5 because of fibrin deposition in placenta. Anticoagulant treatment can prevent this fibrin deposition and extend the survival of embryos; however, no viable EPCR−/− embryos were obtained at E16.5,[46] as EPCR−/− embryos die between E10.5 and E16.5, which overlaps with the period of

migration of HSCs and with the onset of intensive hematopoiesis in FL.[10] The lethality of EPCR$^{-/-}$ embryos may be caused by the impaired engraftment or attachment of HSCs in the perisinusoidal niche in FL. Additional studies are required to fully elucidate the molecular mechanisms involving the cytoprotective function of EPCR in FL HSCs.

We concluded that EPCR^{+} HSCs resided in the APC- and ECM-rich perisinusoidal niche in E12.5 mouse FL. In this perisinusoidal niche, EPCR^{+} HSCs were in a relatively slow cycling state, which was regulated by *p57* and *p18*. Furthermore, the cytoprotective APC/EPCR/Par-1 signaling pathway may be involved in EPCR^{+} HSC maintenance via interaction with other factors to regulate the intrinsic and extrinsic molecular mechanism. Further investigation of the mechanism of interaction between HSCs and the perisinusoidal niche should contribute to the development of efficient ex vivo expansion methods for HSCs, novel therapeutic protocols for HSC transplantation, and artificial generation of HSCs.

Acknowledgments

We appreciate the assistance of Naoko Tago in flow cytometry and Kana Fukushima in animal experiments.

This study was supported in part by the Ministry of Education, Science, Sports and Culture (Grant-in-Aid for Specially Promoted Research, 2008) and the Global Center of Excellence Program of Keio University (Education and Research Center for Stem Cell Medicine).

Authorship

Contribution: H.I. designed and performed experiments, analyzed data, interpreted results, and wrote the paper; F.A. interpreted results, provided guidance for the group, and assisted in manuscript preparation; Y.K. interpreted results and provided guidance for the group; M.D. performed experiments; and T.S. designed experiments, interpreted results, provided guidance for the group, and assisted in manuscript preparation.

Conflict-of-interest disclosure: The authors declare no competing financial interests.

Correspondence: Hiroko Iwasaki or Toshio Suda, Department of Cell Differentiation, The Sakaguchi Laboratory of Developmental Biology, Keio University School of Medicine, 35 Shinanomachi, Shinjuku, Tokyo 160-8582 Japan; e-mail: hiroko-ko@umin.ac.jp or sudato@sc.itc.keio.ac.jp.

References

1. Schofield R. The relationship between the spleen colony-forming cell and the haemopoietic stem cell. *Blood Cells.* 1978;4(1-2):7-25.
2. Yin T, Li L. The stem cell niches in bone. *J Clin Invest.* 2006;116(5):1195-1201.
3. Zhang J, Niu C, Ye L, et al. Identification of the haematopoietic stem cell niche and control of the niche size. *Nature.* 2003;425(6960):836-841.
4. Calvi LM, Adams GB, Weibrecht KW, et al. Osteoblastic cells regulate the haematopoietic stem cell niche. *Nature.* 2003;425(6960):841-846.
5. Arai F, Hirao A, Ohmura M, et al. Tie2/angiopoietin-1 signaling regulates hematopoietic stem cell quiescence in the bone marrow niche. *Cell.* 2004;118(2):149-161.
6. Nilsson SK, Johnston HM, Whitty GA, et al. Osteopontin, a key component of the hematopoietic stem cell niche and regulator of primitive hematopoietic progenitor cells. *Blood.* 2005;106(4):1232-1239.
7. Matrosova VY, Orlovskaya IA, Serobyan N, Khaldoyanidi SK. Hyaluronic acid facilitates the recovery of hematopoiesis following 5-fluorouracil administration. *Stem Cells.* 2004;22(4):544-555.
8. Sugiyama T, Kohara H, Noda M, Nagasawa T. Maintenance of the hematopoietic stem cell pool by CXCL12-CXCR4 chemokine signaling in bone marrow stromal cell niches. *Immunity.* 2006;25(6):977-988.
9. Kiel MJ, Yilmaz OH, Iwashita T, Yilmaz OH, Terhorst C, Morrison SJ. SLAM family receptors distinguish hematopoietic stem and progenitor cells and reveal endothelial niches for stem cells. *Cell.* 2005;121(7):1109-1121.
10. Mikkola HK, Orkin SH. The journey of developing hematopoietic stem cells. *Development.* 2006;133(19):3733-3744.
11. Fukudome K, Esmon CT. Identification, cloning, and regulation of a novel endothelial cell protein C/activated protein C receptor. *J Biol Chem.* 1994;269(42):26486-26491.
12. Laszik Z, Mitro A, Taylor FB Jr, Ferrell G, Esmon CT. Human protein C receptor is present primarily on endothelium of large blood vessels: implications for the control of the protein C pathway. *Circulation.* 1997;96(10):3633-3640.
13. Crawley JT, Gu JM, Ferrell G, Esmon CT. Distribution of endothelial cell protein C/activated protein C receptor (EPCR) during mouse embryo development. *Thromb Haemost.* 2002;88(2):259-266.
14. Galligan L, Livingstone W, Volkov Y, et al. Characterization of protein C receptor expression in monocytes. *Br J Haematol.* 2001;115(2):408-414.
15. Sturn DH, Kaneider NC, Feistritzer C, Djanani A, Fukudome K, Wiedermann CJ. Expression and function of the endothelial protein C receptor in human neutrophils. *Blood.* 2003;102(4):1499-1505.
16. Scheffer GL, Flens MJ, Hageman S, Izquierdo MA, Shoemaker RH, Scheper RJ. Expression of the vascular endothelial cell protein C receptor in epithelial tumour cells. *Eur J Cancer.* 2002;38(11):1535-1542.
17. Stearns-Kurosawa DJ, Kurosawa S, Mollica JS, Ferrell GL, Esmon CT. The endothelial cell protein C receptor augments protein C activation by the thrombin-thrombomodulin complex. *Proc Natl Acad Sci U S A.* 1996;93(19):10212-10216.
18. Mosnier LO, Zlokovic BV, Griffin JH. The cytoprotective protein C pathway. *Blood.* 2007;109(8):3161-3172.
19. Cheng T, Liu D, Griffin JH, et al. Activated protein C blocks p53-mediated apoptosis in ischemic human brain endothelium and is neuroprotective. *Nat Med.* 2003;9(3):338-342.
20. Mosnier LO, Griffin JH. Inhibition of staurosporine-induced apoptosis of endothelial cells by activated protein C requires protease-activated receptor-1 and endothelial cell protein C receptor. *Biochem J.* 2003;373(Pt 1):65-70.
21. Riewald M, Petrovan RJ, Donner A, Mueller BM, Ruf W. Activation of endothelial cell protease activated receptor 1 by the protein C pathway. *Science.* 2002;296(5574):1880-1882.
22. Feistritzer C, Riewald M. Endothelial barrier protection by activated protein C through PAR1-dependent sphingosine 1-phosphate receptor-1 crossactivation. *Blood.* 2005;105(8):3178-3184.
23. Akashi K, He X, Chen J, et al. Transcriptional accessibility for genes of multiple tissues and hematopoietic lineages is hierarchically controlled during early hematopoiesis. *Blood.* 2003;101(2):383-389.
24. Balazs AB, Fabian AJ, Esmon CT, Mulligan RC. Endothelial protein C receptor (CD201) explicitly identifies hematopoietic stem cells in murine bone marrow. *Blood.* 2006;107(6):2317-2321.
25. Kent DG, Copley MR, Benz C, et al. Prospective isolation and molecular characterization of hematopoietic stem cells with durable self-renewal potential. *Blood.* 2009;113(25):6342-6350.
26. Zwicky C, Gerber S, Gasparini D, et al. Preparation and analysis of fetal liver extracts. *Bone Marrow Transplant.* 2000;26(6):667-671.
27. Fernandez JA, Xu X, Liu D, Zlokovic BV, Griffin JH. Recombinant murine-activated protein C is neuroprotective in a murine ischemic stroke model. *Blood Cells Mol Dis.* 2003;30(3):271-276.
28. Sato T, Onai N, Yoshihara H, Arai F, Suda T, Ohteki T. Interferon regulatory factor-2 protects quiescent hematopoietic stem cells from type I interferon-dependent exhaustion. *Nat Med.* 2009;15(6):696-700.
29. Carreira CM, Nasser SM, di Tomaso E, et al. Lyve-1 is not restricted to the lymph vessels: expression in normal liver blood sinusoids and down-regulation in human liver cancer and cirrhosis. *Cancer Res.* 2001;61(22):8079-8084.
30. Spangrude GJ, Johnson GR. Resting and activated subsets of mouse multipotent hematopoietic stem cells. *Proc Natl Acad Sci U S A.* 1990;87(19):7433-7437.
31. Wolf NS, Kone A, Priestley GV, Bartelmez SH. In vivo and in vitro characterization of long-term repopulating primitive hematopoietic cells isolated by sequential Hoechst 33342-rhodamine 123 FACS selection. *Exp Hematol.* 1993;21(5):614-622.
32. Uchida N, Dykstra B, Lyons K, Leung F, Kristiansen M, Eaves C. ABC transporter activities of murine hematopoietic stem cells vary according to their developmental and activation status. *Blood.* 2004;103(12):4487-4495.
33. Drouin R, Lemieux N, Richer CL. Analysis of DNA replication during S-phase by means of dynamic chromosome banding at high resolution. *Chromosoma.* 1990;99(4):273-280.
34. Merkel DE, Dressler LG, McGuire WL. Flow cytometry, cellular DNA content, and prognosis in human malignancy. *J Clin Oncol.* 1987;5(10):1690-1703.

35. Gerdes J, Li L, Schlueter C, et al. Immunobiochemical and molecular biologic characterization of the cell proliferation-associated nuclear antigen that is defined by monoclonal antibody Ki-67. *Am J Pathol.* 1991;138(4):867-873.

36. Ekholm SV, Reed SI. Regulation of G(1) cyclin-dependent kinases in the mammalian cell cycle. *Curr Opin Cell Biol.* 2000;12(6):676-684.

37. Breviario F, Caveda L, Corada M, et al. Functional properties of human vascular endothelial cadherin (7B4/cadherin-5), an endothelium-specific cadherin. *Arterioscler Thromb Vasc Biol.* 1995;15(8):1229-1239.

38. Kim I, Saunders TL, Morrison SJ. Sox17 dependence distinguishes the transcriptional regulation of fetal from adult hematopoietic stem cells. *Cell.* 2007;130(3):470-483.

39. Ema H, Nakauchi H. Expansion of hematopoietic stem cells in the developing liver of a mouse embryo. *Blood.* 2000;95(7):2284-2288.

40. Enzan H, Himeno H, Hiroi M, Kiyoku H, Saibara T, Onishi S. Development of hepatic sinusoidal structure with special reference to the Ito cells. *Microsc Res Tech.* 1997;39(4):336-349.

41. Lange AW, Keiser AR, Wells JM, Zorn AM, Whitsett JA. Sox17 promotes cell cycle progression and inhibits TGF-beta/Smad3 signaling to initiate progenitor cell behavior in the respiratory epithelium. *PLoS ONE.* 2009;4(5):e5711.

42. Hock H, Hamblen MJ, Rooke HM, et al. Gfi-1 restricts proliferation and preserves functional integrity of haematopoietic stem cells. *Nature.* 2004;431(7011):1002-1007.

43. Rudini N, Felici A, Giampietro C, et al. VE-cadherin is a critical endothelial regulator of TGF-beta signalling. *EMBO J.* 2008;27(7):993-1004.

44. Finigan JH, Dudek SM, Singleton PA, et al. Activated protein C mediates novel lung endothelial barrier enhancement: role of sphingosine 1-phosphate receptor transactivation. *J Biol Chem.* 2005;280(17):17286-17293.

45. Van Sluis GL, Niers TMH, Esmon CT, et al. Endogenous activated protein C limits cancer cell extravasation through sphingosine-1-phosphate receptor 1-mediated vascular endothelial barrier enhancement. *Blood.* 2009;114(9):1968-1973.

46. Gu J-M, Crawley JTB, Ferrell G, et al. Disruption of the endothelial cell protein C receptor gene in mice causes placental thrombosis and early embryonic lethality. *J Biol Chem.* 2002;277(45):43335-43343.